Rev. Mexicana Astron. Astrof., **23**, 171-179 (1992)

THE OPACITY PROJECT — RESULTS FOR OPACITIES

Yu Yan

Department of Astronomy
University of Illinois

RESUMEN. Se discuten los métodos y resultados del Proyecto de la Opacidad. Se presenta una librería de opacidades para mezclas arbitrarias.

ABSTRACT. Methods and results of the Opacity Project are discussed. An emerging opacity library for arbitrary compositions is presented.

Key words: OPACITIES

1 INTRODUCTION

The calculation of stellar opacities is a substantial undertaking. It requires a realistic equation of state that adequately predicts the ionisation equilibrium of a multi-component plasma as well as the occupation of spectroscopic bound states, a large amount of atomic data of considerable accuracy and completeness, and line-broadening parameters which are at least statistically accurate.

In previous calculations of opacities (see Cox 1965, Cox and Tabor 1976, Hüebner 1985; Carson, Mayers and Stibbs 1968, Carson 1976) the atomic data were obtained from simple, drastic approximations; the uncertainties in the opacity due to these approximations have not been systematically examined until recently. In an effort to reconcile the discrepancies between the standard Cepheid models and observation Simon (1982) suggested that the heavy element contribution to the opacity might have been under-estimated by a factor of 2–3. The Opacity Project (OP) was initiated in direct response to his plea for a re-examination of heavy element opacities (Seaton 1987); atomic radiative data for all ionisation stages of the astrophysically abundant elements were calculated using the close-coupling method (Berrington *et al.* 1987, Seaton *et al.* 1991) and related "top-up" procedures. Another major effort at re-examining heavy element opacities is the OPAL project at Lawrence Livermore National Laboratory (Iglesias, Rogers and Wilson 1987, 1990). In this paper we describe the methods used in the OP calculation of stellar opacities, and present our results in a format for easy comparison with those of OPAL.

In the Opacity Project we take the long-term view of providing a user-oriented, publicly accessible opacity library for the astrophysical community. The pioneering work in this area is the Los Alamos Astrophysical Opacity Library (LAAOL, Hüebner *et al.* 1977), which, for nearly 15 years, has been the standard (and the only) source of opacities of arbitrary composition. Here we describe an alternative opacity library, as an integral part of the OP production results, which will offer significant improvements over LAAOL. Some of the improvements (such as better frequency resolution, finer grids for interpolation in temperature and density) are related to the increased computer power and storage capacity in the past ten years; others are entirely due to improvements in the atomic model.

2 COMPUTATIONAL METHODS

The monochromatic opacity contains the bound-bound contribution

$$\kappa_\nu(a \to b) = \frac{\pi e^2}{mc} N_a f(b,a) \phi_\nu \tag{2.1}$$

and the bound-free contribution

$$\kappa_\nu = N_a \sigma_a(\nu). \tag{2.2}$$

Equations (2.1) and (2.2) illustrate the main parts of the opacity calculation: the occupation number N_a of a state a is given by the equation of state (EOS); the oscillator strength $f(b,a)$ for a bound-bound transition $a \to b$ and the cross section σ_a for photo-ionisation from state a are obtained from the atomic model; the line-profile factor ϕ_ν, normalised to

$$\int \phi_\nu d\nu = 1, \tag{2.3}$$

must be computed for each spectral line. Other processes contributing to the monochromatic opacity are free-free absorption and photon scattering by electrons and atoms.

We use the MHD equation of state (Hummer and Mihalas 1988, Mihalas, Däppen and Hummer 1988) to determine the ionisation equilibrium and the population of the internal atomic states. It is based on the free energy minimisation method, and includes non-ideal terms due to partial electron degeneracy and Coulomb interactions among all charged particles. The internal partition function is modified by an occupation probability factor, which takes into account the perturbation by plasma ions or neutral particles. It should be clear that the notion of spectroscopic levels of an atom or ion—an essential starting point for modelling stellar envelope opacities—has a direct equivalence in the EOS under such a chemical picture.

We use atomic data calculated in the close-coupling (CC) approximation, where the wave function Ψ of an $(N+1)$-electron ion or atom is given by the expansion

$$\Psi = \mathcal{A} \sum_i \phi_i^{(N)} \theta_i + \sum_j \Phi_j^{(N+1)}. \tag{2.4}$$

In (2.4) $\mathcal{A}$ is the anti-symmetrisation operator, $\phi_i^{(N)}$ are the wave functions for the N-electron target, θ_i are the orbital functions of the colliding electron, and $\Phi_j^{(N+1)}$ are optimised bound-type functions for the $(N+1)$-electron system.

When (2.4) is applied to a bound state, we classify the dominant channel in the expansion schematically as Tnl or C, and designate the energy level accordingly. A Tnl state arises from the first sum in (2.4); a C state has all electrons in the ground complex, and may arise from the first or the second sum in (2.4). For iso-electronic sequences H–Mg the OP atomic data are usually such that the C states of one ion constitute the T states of the next one (the ion with one more electron). For systems with more electrons (particularly Fe VIII–XII) some compromise had to be made in truncating the eigenfunction expansion corresponding to the first sum in (2.4); a "top-up" procedure was developed to augment the previously truncated T (and therefore Tnl) states of an N-electron target from the C states of the $(N-1)$-electron target (Seaton *et al.* 1991). We shall refer to these additional data as PLUS data.

The LS coupling scheme was assumed in the calculation of the atomic data. For selected Fe ions the effect of fine structure (FS) splitting has been investigated using the Landé interval rule and Racah algebra. The issue of FS splitting on the opacity will be discussed in §4.

We use line-broadening methods developed by Seaton (references are given in Seaton *et al.* 1991). The line-profile parameters for non-hydrogenic ions were obtained from a best fit to results of accurate CC calculations for selected transitions in the electron-impact approximation. For hydrogenic systems broadening due to electron perturbers was treated using quantum-mechanical methods, and the Stark splittings due to the ion microfield were calculated allowing for line dissolution.

The Rosseland mean opacity κ_R is given by

$$\kappa_R^{-1} \int_0^\infty g(u)du = \int_0^\infty \frac{1}{\kappa(u)} g(u)du, \tag{2.5}$$

where $u = h\nu/kT$, $\kappa(u)$ is the monochromatic opacity (corrected for stimulated emission), and $g(u)$ is a weighting function,

$$g(u) = u^4 e^{-u}(1 - e^{-u})^{-2}. \tag{2.6}$$

The integrals in (2.5) are computed in the range $-2.5 \leq \log_{10} u \leq 1.5$ on a frequency mesh of typically 10^5 points.

The opacity code incorporating the methods and data (except PLUS data) described thus far has been developed at the National Center for Supercomputing Applications (NCSA). For the purpose of checking the computational algorithms and studying the sensitivity of various parameters in the theory, a second opacity code was developed at University College London (UCL), which used the same atomic data and line-broadening methods but a somewhat simplified EOS. Extensive cross-checks were made using the two codes, ranging from detailed tests of mean and monochromatic opacities for single elements to a systematic comparison of a full opacity table for the King IVa mixture. The level of agreement we obtained was such as to give us confidence that no major coding error flawed the opacity calculations. (The King IVa abundances were considered in order to compare with previous works; see Cox and Tabor 1976.) In the final production work the NCSA code will be used.

3 DISCUSSION AND SELECTED RESULTS

3.1 Discussion

Not all absorption processes contribute equally significantly to the opacity at a given temperature and density. Apart from the obvious factor of elemental abundances, the two mechanisms that select the contributing processes are the ionisation equilibrium and the weighting function (2.6). As the temperature increases, the ionisation balance for a given element shifts towards higher stages of ionisation, while the window of the weighting function (which peaks at about $h\nu = 4kT$) shifts towards higher photon energies. The combined effect is to map out a region of the absorption atlas favoured by the opacity. Clearly the region is not sharply defined, as density effects also tend to spread the ionisation balance; however, some knowledge of the interplay between the EOS and the atomic transitions is useful as a guide for understanding the opacity spectrum and for further improvements on the atomic data.

First consider opacities for a single element, Fe. At $\log T = 4.5$ ($kT = 0.2$ Ryd.) Fe is mostly 0–5 times ionised. The window corresponding to (2.6) selects a photon energy range such that $\Delta n = 0$ transitions in these ions are most heavily weighted. Thus the important lines are those due to $C \rightarrow C'$ and $T\,nl \rightarrow T\,nl'$ transitions. At $\log T = 5.5$ Fe is mostly 8–16 times ionised, and the dominant contribution to the opacity comes from ion stages IX–XIII. Both $\Delta n = 0$ and 1 transitions in these ions are heavily weighted by the opacity window. Thus, for example, lines due to $C \rightarrow T\,nl$ ($n = 4$) transitions now become important. At $\log T = 6.5$ Fe is mostly H- to O-like, and the opacity window selects transitions $\Delta n = 1$, 2 etc.

The above outline can readily be extended to photo-ionisation. Here we shall restrict the discussion to PEC resonances, which are characterised by broad features in the cross sections (Yu Yan and Seaton 1987). We write the PEC resonance schematically as $T\,nl \rightarrow T'\,nl$, where $T\,nl$ is a bound state and $T'\,nl$ an auto-ionising state. The position of the resonance corresponds to the energy of the transition $T \rightarrow T'$ in the core (the ion with one less electron). Thus to return to opacities for Fe, the PEC resonances of interest are due to core transitions $T \rightarrow T'$ where

$\log T = 4.5$	Fe^{1-6+}	T and T' are close in energy (e.g. in the same complex);
5.5	Fe^{9-17+}	T and T' are such that $\Delta n = 0$ or 1 (e.g. 3 to 3, 3 to 4);
6.5	Fe^{19-25+}	T and T' are such that $\Delta n = 1$ or 2 (e.g. 2 to 3, 2 to 4).

It should be noted that the energies of the above transitions are based on single-electron excitation, and that the schematic designations of levels sometimes break down in the lowest ionisation stages.

Now consider opacities for a mixture. We take the King IVa mix and include elements up to iron; it gives a neon abundance which is considered rather too high (Auer and Mihalas 1973), but will otherwise suffice as a general illustration. Figures 1(a–c) show the Rosseland mean opacity as successive groups of elements in the mixture are included. At $\log T = 4.5$ (a) the dominant contribution to the opacity comes from H and He. Inclusion of C, N and O can increase the opacity by some 10%, and inclusion of Fe can further increase the opacity by some 30%. At $\log T = 5.5$ (b) the opacity is dominated by contributions from metals, notably Fe and (Li- to B-like) Ne, and, at the lowest densities, by electron scattering. At $\log T = 6.5$ (c) and at relatively high densities where the opacity is not dominated by electron scattering, Ne (now H- and He-like) again makes a large contribution; the Fe contribution is also significant, but is somewhat diminished compared to Figure 1b.

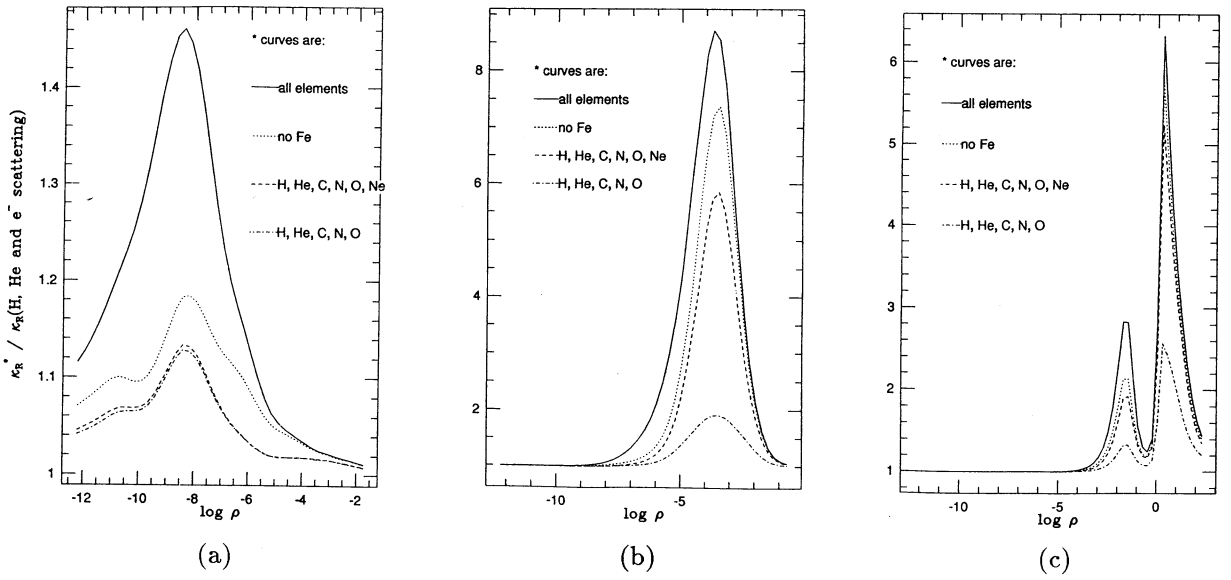

FIG. 1.—Ratio of Rosseland mean opacities due to inclusion of successive groups of elements to those of hydrogen, helium and electron scattering, in the King IVa mixture, for log T = (a) 4.5, (b) 5.5, (c) 6.5.

The calculations for Fe (solid curves) were made without allowance for the PLUS Tnl states. Inclusion of the PLUS data may further enhance the Fe peak of (b), but will have rather modest effects on (a) and (c).

3.2 Selected results

Here we consider the mixture with $X = 0.7$, $Z = 0.2$ and "AG abundances" (Anders and Grevesse 1989) including elements up to iron, and compare opacities obtained using the UCL code and the PLUS data with the OPAL opacities (Rogers and Iglesias 1991) at selected values of the density variable $R = \rho/T_6^3$, where T_6 is the temperature in 10^6K.

Figures 2(a–e) show the Rosseland mean as a function of $\log T$. A common feature of these figures is the successive bumps in the opacity for $\log T$: (i) below 4.5, (ii) between 4.5 and 5, (iii) above 5. Without too much simplification the bumps can be attributed to hydrogen, helium and metal contributions, respectively, and will be referred to as the X-, Y- and Z-bumps.

In the region of the X- and Y-bumps the OP and OPAL opacities agree within (and usually much better than) 10%. This is encouraging, but should not be surprising, since the atomic models for the dominant processes of this region are similar in the two calculations.

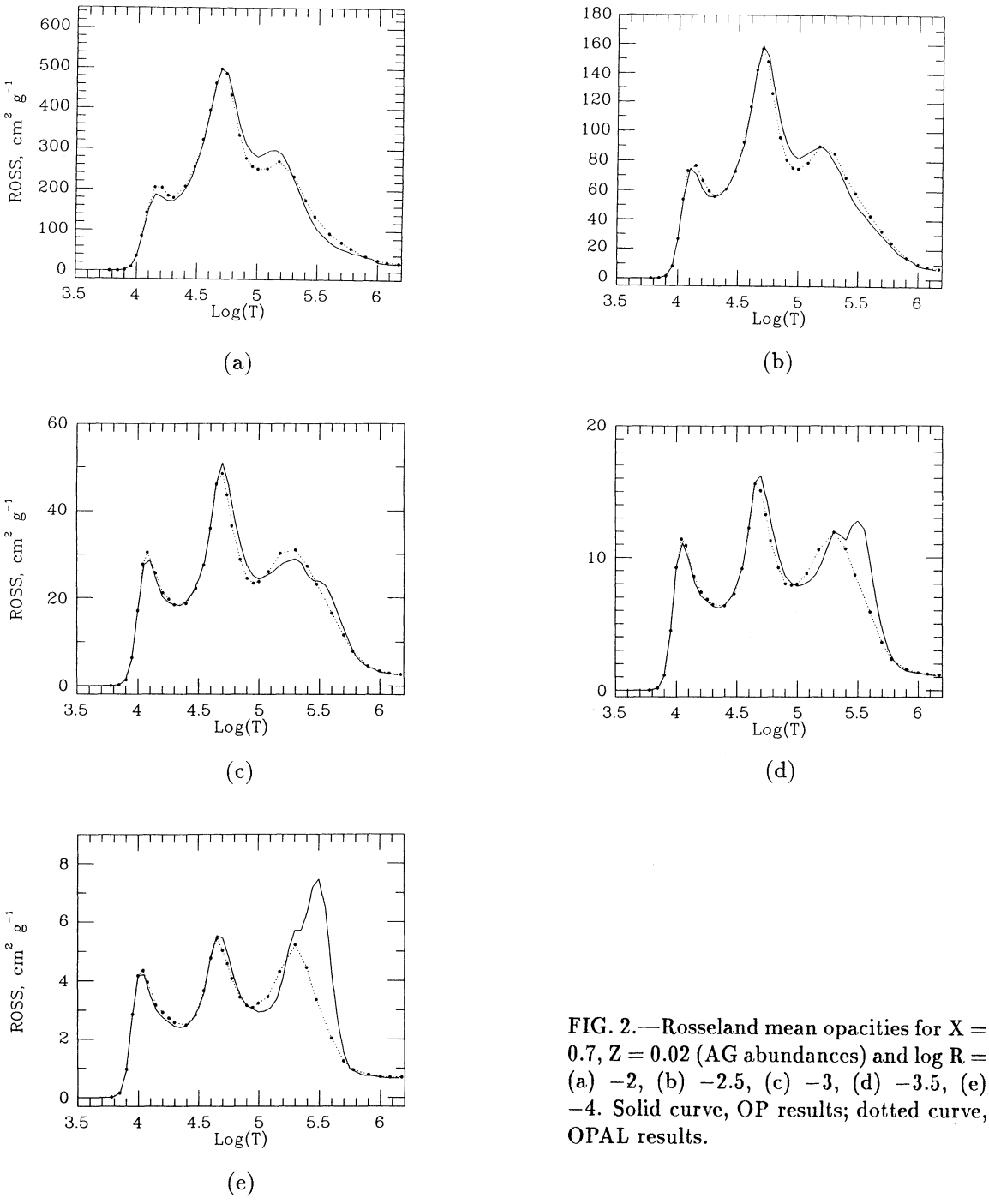

FIG. 2.—Rosseland mean opacities for X = 0.7, Z = 0.02 (AG abundances) and log R = (a) −2, (b) −2.5, (c) −3, (d) −3.5, (e) −4. Solid curve, OP results; dotted curve, OPAL results.

In the region of the Z-bump the OP and OPAL calculations used quite different atomic models. At high densities (a–c) the qualitative agreement in the opacity is fairly good. The shapes and the magnitudes of

the Z-bump are somewhat different. At lower densities (d, e) the OP Z-bump develops a second component, giving opacities that are significantly higher than those of OPAL at certain temperatures.

There are many absorption processes which contribute to the opacity in the region of the Z-bump. At the time of this workshop we have not yet pinpointed the sources for the detailed differences in the OP and OPAL results. Futher work is needed to more precisely specify the shape and the magnitude of the Z-bump. A list of possible uncertainties in the current opacities is given in §4; here we only note the following:

(i) in the vicinity of the Z-bump both the OP and the OPAL opacities are substantially larger than the early opacities (e.g. LAAOL);

(ii) in computing the OP opacities of Figs. 2(a–e), though allowance was made for some PLUS states of the Fe ions, not all the absorption processes described in §3.1 were fully included (e.g. some PEC resonances and $C \rightarrow T\,nl$ transitions were omitted).

4 UNCERTAINTIES IN THE CURRENT ATOMIC OPACITIES

The OP and OPAL calculations of stellar opacities represent two different approaches to the atomic physics problem. In OP a rather sophisticated atomic model is used to generate accurate transition data, but the database must be gauged (and augmented) for completeness by the method outlined in §3.1 and by convergence in the mean opacity. In OPAL a simpler, single-configuration atomic model is used to generate all transition data of interest at a given matter condition; the uncertainties due to configuration interaction (CI), however, cannot be assessed independently. The present agreement between the two calculations is a remarkable step towards eliminating serious errors in stellar opacities. To help further reduce the uncertainties, we discuss several approximations used in the OP and OPAL methods.

4.1 Rydberg resonances

In OP resonances retain their correct quantum-mechanical profiles. Pressure broadening of resonances has been examined separately, but has not been incorporated into the opacity calculation.

In OPAL resonances are treated as spectral lines. The interference effect due to continuum interaction is not taken into account, but plasma effects, particularly line broadening, are fully included.

The relative importance of the plasma and the continuum interaction effects depends on the pressure broadening width compared to the resonance profile width.

4.2 PEC *resonances*

In OP photo-excitation of the core is treated in a fully quantum-mechanical manner. Because of the interaction between the core and the spectator electron the PEC resonance width is usually much larger than the Rydberg resonance width, and plasma broadening is unlikely to be important. However, some PEC processes are omitted in the opacity calculation; more work is needed to complete the database.

In OPAL PEC resonances are again treated as spectral lines. All PEC processes are included, but the broadening mechanisms and the form of the profile are inadequate. Furthermore, Hibbert shows that neglect of CI may sometimes introduce errors due to spurious oscillator strengths of the core transitions (see Seaton *et al.* 1991).

PEC resonances provide an enhanced continuum background for the main absorption lines of the core ion. To control the uncertainties in atomic opacities, it is necessary to include all important PEC processes in a scheme which allows for the correct broadening mechanisms.

4.3 Fine structure and intermediate coupling

Subsidiary OP calculation indicates that inclusion of FS splitting can increase the Rosseland mean for iron by some 60%. Although this corresponds to an increase of less than 10% for the solar mixture, neglect of such an effect is undoubtedly a source of uncertainty, particularly for iron-rich compositions.

Fine structure is important when the FS separations are larger than the line widths. For conditions

near the Z-bump this criterion is easily satisfied in the Fe ions.

Inclusion of inter-combination (IC) lines can further increase the opacity. Preliminary calculation indicates that many IC lines for the Fe ions of interest have f-values of about one-tenth of those for allowed lines.

It is planned to include in future OP work FS splitting and IC lines obtained from large atomic structure calculations for selected ions.

4.4 The iron group

The cosmic abundance of nickel is about 5% of that of iron. With absorption properties similar to iron, it is plausible that nickel may significantly alter the Z-bump in some temperature-density domains. It is planned to include nickel at a later stage of the OP work.

5 THE OPACITY LIBRARY

The computation of opacities from the basic absorption processes is a CPU-intensive affair. A large number of radiative transitions must be considered, and profile factors must be calculated for all individual lines. It is a task that cannot easily be relegated to the end-user.

A strategy emerged during the OP development work which enabled a two-step design for the opacity code, separating the production of results from the basic absorption processes. It was postulated, and later verified numerically, that to a sufficiently good approximation the statistical-mechanical properties of a chemical element k is independent of the plasma composition at a given *electron density* N_e. The distribution of the atomic states and the ionisation equilibrium, and hence the monochromatic opacity, are taken to be invariant to the mixture composition for each set of (T, N_e, k).

In practice we compute *single element* monochromatic opacities using occupation numbers from the solar mixture. The monochromatic opacities are packed to a specified accuracy (usually 0.01), and archived on a standard $(\log T, \log N_e, k)$ grid. Numerical experimentation suggested that a grid with $\Delta \log T = 0.025$, $\Delta \log N_e = 0.25$ allowed accurate interpolation in the mean opacities. Thus we take

$$3.5 \leq \log T \leq 7.2, \qquad \Delta \log T = 0.025, \qquad \Delta \log N_e = 0.25$$

and lower, upper limits for $\log N_e$ varying with $\log T$. For this grid and 14 chemical elements the amount of monochromatic opacity data after packing is about 12 gigabytes.

Constructing the opacity spectrum for a mixture is now a separate (and trivial) step. The monochromatic opacities for the elements in the mixture can be summed directly, weighted by the relative abundances. User codes have been developed to mix the elements and to produce the Rosseland and the Planck means, multi-group means, the opacity distribution function, and the mixture spectrum. Interpolation of mean opacities can be in either the electron density or the mass density.

The archive of single element monochromatic opacities and the user codes form the *Opacity Library.*

The Opacity Library is conceptually similar to LAAOL. The former uses a finer spectrum resolution, a better grid for interpolation, and therefore contains a much larger amount of data. More importantly, it uses radiative data obtained from a much better atomic model. Figure 3(a) compares the pure carbon monochromatic opacities at one tabular point in LAAOL to what the Opacity Library would contain at the same temperature and density (lower and middle plots). It can be seen that the two spectra differ substantially in the number and the strength of lines and in the resonance structure of the continuum. The effect of PEC resonances at $u = 3.2, 4.3, 5.2$ etc. in the Opacity Library spectrum is most clearly seen in the Rosseland integrand (upper plot); these PEC features are entirely missing in LAAOL. Figure 3(b) compares the pure iron monochromatic opacities at another tabular point in LAAOL. Because of the structural complexity of the Fe ions, improvements in the atomic model result in large differences in the opacities.

It is planned to make the Opacity Library publicly available at a later stage of the OP work.

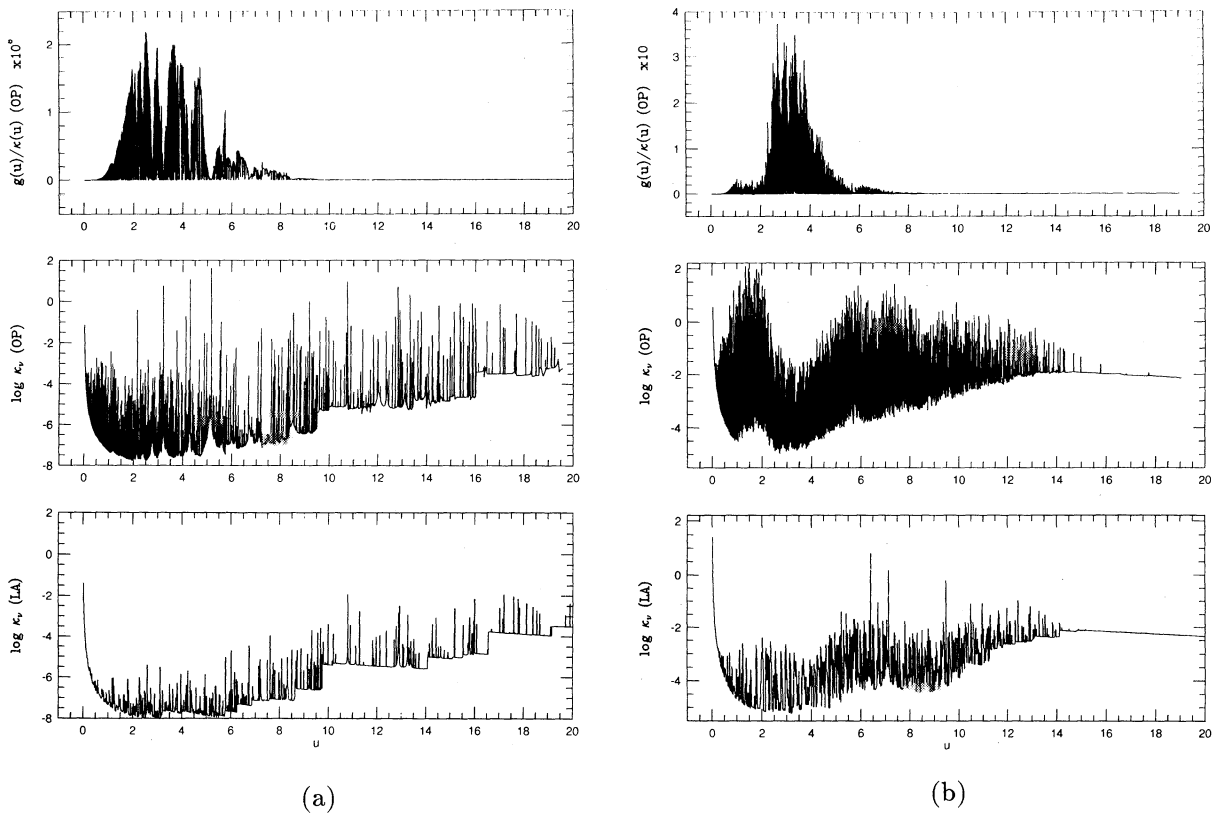

FIG. 3—Monochromatic opacities from LAAOL and OP (lower, middle plots respectively) and the corresponding OP Rosseland integrand (upper plot) for (a) pure carbon at log T = 4.463, log ρ = −8.03 and (b) pure iron at log T = 5.542, log ρ = −5.24.

ACKNOWLEDGEMENT

Other members of the OP involved in the opacity calculations are D.M. Mihalas, A.K. Pradhan and M.J. Seaton.

We thank F.J. Rogers and C.A. Iglesias for providing data for comparison in advance of publication.

Work supported by National Science Foundation grants AST85-19209 and AST89-14143, and by unrestricted research funds from the University of Illinois.

REFERENCES

Anders, E. and Grevesse, N. 1989, *Geochim. Cosmochim Acta.*, **53**, 197.
Auer, L.H. and Mihalas, D. 1973, *Ap. J.*, **184**, 151.
Berrington, K.A., Burke, P.G., Butler, K., Seaton, M.J., Storey, P.J., Taylor, K.T. and Yu Yan 1987, *J. Phys. B: At. Mol. Phys.*, **20**, 6379.
Carson, T.R. 1976, *Ann. Rev. Astron. Astrophys.*, **14**, 95.
Carson, T.R., Mayer, D.F. and Stibbs, D.W.N. 1968, *Mon. Not. R. astr. Soc.*, **140**, 483.
Cox, A.N. 1965, in *Stars and stellar systems*, ed. L. H. Aller and D. B. Laughlin (Chicago: Chicago University

Press), p195.
Cox, A.N. and Tabor, J.E. 1976, *AP. J. Supp.*, **31**, 271.
Hüebner, W.F. 1985, in *Physics of the sun* ed. P. Sturrock, T. Holzer, D. Mihalas and R. Ulrich (Dordrecht: Reidel), p33.
Hüebner, W.F., Merts, A.L., Magee, N.H.Jr. and Argo, M.F. 1977, *Astrophysical Opacity Library*, Los Alamos Scientific Laboratory Report LA-6760-M.
Hummer, D.G. and Mihalas, D.M. 1988, *Ap. J.*, **331**, 794.
Iglesias, C.A., Rogers, F.J. and Wilson, B.G. 1987, *Ap. J. (letters)*, **322**, L45.
— 1990, *Ap. J.*, **360**, 221.
Mihalas, D.M., Däppen, W. and Hummer, D.G. 1988, *Ap. J.*, **331**, 815.
Rogers, F.J. and Iglesias, C.A 1991, preprint.
Seaton, M.J. 1987, *J. Phys. B: At. Mol. Phys.*, **20**, 6363.
Seaton, M.J., Zeippen, C.J., Tully, J.A., Pradhan, A.K., Mendoza, C., Hibbert, A. and Berrington, K.A. 1991, this volume.
Simon, N.R. 1982, *Ap. J.*, **260**, L87.
Yu Yan and Seaton, M.J. 1987, *J. Phys. B: At. Mol. Phys.*, **20**, 6409.

Yu Yan: Department of Astronomy, University of Illinois, 1002 West Green Street, Urbana, Illinois 61801, U.S.A.